Application of a liquid crystal spatial light modulator to laser marking

Application of a liquid crystal spatial light modulator to laser marking

Jonathan P. Parry,* Rainer J. Beck, Jonathan D. Shephard, and Duncan P. Hand

Heriot-Watt University, School of Engineering and Physical Sciences, Riccarton, Edinburgh, EH14 4AS, UK

*Corresponding author: J.Parry@hw.ac.uk

Received 19 November 2010; revised 17 March 2011; accepted 17 March 2011;
posted 21 March 2011 (Doc. ID 138502); published 18 April 2011

Laser marking is demonstrated using a nanosecond (ns) pulse duration laser in combination with a liquid crystal spatial light modulator to generate two-dimensional patterns directly onto thin films and bulk metal surfaces. Previous demonstrations of laser marking with such devices have been limited to low average power lasers. Application in the ns regime enables more complex, larger scale marks to be generated with more widely available and industrially proven laser systems. The dynamic nature of the device is utilized to improve mark quality by reducing the impact of the inherently speckled intensity distribution across the generated image and reduce thermal effects in the marked surface.

OCIS codes: 110.1080, 140.3390, 350.3390, 350.3850.

1. Introduction

For many laser machining applications it is common to use some form of beam shaping to modify the typically Gaussian intensity distribution of the laser to an intensity profile that is more appropriate for the task. For example, refractive optics [1,2] may be used to generate top hat intensity distributions, which are better suited to drilling applications or more complex profiles may be generated to mark patterns on a surface either with diffractive elements or masks [3–6]. Dynamic beam shaping elements offer an advantage in terms of changing between shapes rapidly to quickly mark or machine a series of features across a surface or even to modify the beam shape during a machining operation.

Deformable mirrors represent one approach to dynamic beam shaping and have the advantage of being a robust technology with a fast response rate (up to ~1 kHz). These devices are well suited to some applications [7,8]; however, they are generally limited in terms of the complexity of beam shaping that they can provide, with commercially available items typically using 37 (hexagonally close packed) active elements. While some devices with higher numbers of actuators are available (for example, in applications in astronomy [9]), they are prohibitively expensive for laser machining applications.

In this work we present the application of a liquid crystal spatial light modulator (SLM) as a variable diffractive element to provide beam shaping as part of an ns laser machining system. This is a liquid crystal based device working in reflection and although the response rate is slower (75 Hz) compared to a deformable mirror, the device provides a high-resolution phase modification enabling arbitrary beam shapes in the Fourier plane to be generated and modified at will.

Digital micromirror devices represent a further beam shaping technology, which, like liquid crystal SLMs, have been developed for display applications. Such devices consist of an array of tilting micromirrors, which in effect can turn elements of the illumination source on or off by reflecting light toward the imaging optics or to a beam dump. Such devices have been used for laser materials processing [10,11], although they are not widely commercially available as independent units.

Liquid crystal devices have been used for a number of applications, including laser stereo-photolithography

0003-6935/11/121779-07$15.00/0

[12], programmable lenses and filters [13], optical tweezers [14,15], and adaptive optics [16]. Laser machining has also been demonstrated with similar liquid crystal based devices in the femtosecond [17,18] and picosecond [19] regimes where very high peak powers but low average powers are typical, and in the ns regime at relatively low average powers [20,21]. Machining in the ns regime generally involves much higher average powers, which enables higher processing rates with more reliable, industrially proven laser systems. However, this is challenging for a liquid crystal device, which becomes sensitive to high average powers. One potential solution to overcome power handling issues is to address the SLM with a lower power laser beam and add an optical amplifier stage after the device to reach power levels sufficient for machining [22]. However, such a complex arrangement is only worth consideration in the case that other simpler solutions cannot be implemented to increase power handling. In other work we have demonstrated techniques to improve on the power handling capability of the device as well as other issues, such as the inherent curvature of the device [23].

One undesirable feature typical of holograms generated with diffractive elements is the speckled intensity distribution across the image, and here the dynamic nature of the SLM opens up possibilities to improve upon this. A number of techniques have been applied to tackle this problem, particularly in display applications [24,25] where ferroelectric devices are generally used due to their faster response rate. A particularly effective technique first presented by Golan and Shoham [26] is applied here to improve the quality of laser-machined features.

2. Machining with SLM

The SLM used in this work is an LC-R 2500 from Holoeye. This is a liquid crystal based device originally designed for display applications and, hence, has a maximum frame rate of 75 Hz (with a typical response time of 16 ms) and a resolution of 1024 × 768 pixels in a dimension of 19.5 × 14.6 mm. The electronics have been fabricated onto a silicon chip, which is coated with a reflective metallic layer giving a fill factor of >93%. A twisted nematic liquid crystal has then been applied to this. The exact materials used are not disclosed by the manufacturer, but will have been chosen to give good performance across the visible spectrum. No dialectic layers have been included to either enhance reflection of the reflective layer or to minimize reflections from the glass surface. In the off state, the poles of the liquid crystals are aligned parallel to the plane of the display creating a birefringent optical medium. The alignment of the crystals at the back plane of the display is at 45 deg with respect to those at the front, creating a twist of the birefringent axis through the material. As a voltage is applied across a pixel, the crystals are rotated such that the birefringence of the device is reduced until all the crystals are aligned perpendicular to the plane of the device and no birefringence is perceived by normally incident light. Each pixel may introduce a variable phase delay of between 0 and 2π rad to suitably polarized incident light in the visible spectrum.

Based on the manufacturers' recommendations, the total average power handling capability is approximately 3 W for a 14 mm diameter beam. In other work we have demonstrated a power handling capability of 14.7 W limited by the laser output and demonstrated techniques to reduce the effects of the inherent curvature and flickering of the device [23]. The power handling was achieved by mounting the device on a heat sink to reduce the buildup of heat within the device, see Fig. 1. The same laser system, a Spectra-Physics Inazuma, is used again here. This is a frequency-doubled (532 nm), diode-pumped Nd:YVO_4 system operated at 15 kHz repetition rate giving a pulse duration of approximately 60 ns and an average power of 12 W. This gives the highest possible peak intensity from this system, although higher average powers are available at higher repetition rates.

For laser machining, the SLM was incorporated into a 6-f optical system as illustrated in Fig. 1. The beam from the laser was expanded to approximately 14 mm diameter by one telescope (not shown in figure) in order to fill the SLM. A wave plate aligned the linear polarization state of the laser beam to maximize the phase modulation produced by the device. A second telescope after the SLM was aligned to produce a 10 mm collimated beam matched to the design requirements of the scan head. At the intermediate (2-f) focal point of this telescope the desired image is generated, whereas at the back focal plane (4-f) the intensity distribution in the beam reverts to a spatial frequency distribution. The final lens in the system is the flat-field lens of the scan head, and at the focus of this lens (6-f) the final image is produced. The scan head enables the image to be easily positioned or scanned across the workpiece.

Initial machining was carried out on thin aluminum films coated onto glass slides. Because of the relatively large scale of the images produced (~500 μm compared to ~10 μm for a focused Gaussian beam), dwell times of between one and a few hundred milliseconds are required to achieve marks on the

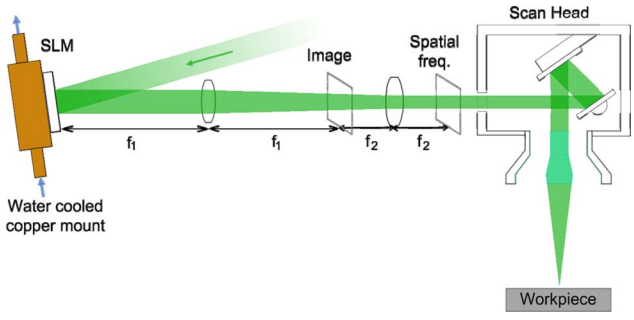

Fig. 1. SLM and optical system to deliver image to workpiece.

surface as a result of the low intensity. This equates to a range of between 20 and a few thousand pulses per mark, depending on the size and material.

Two well-known limitations of diffraction holograms of this type are the prominence of the zero diffraction order and the speckled intensity distribution across the image. The simplest way to avoid the effects of the zero diffraction order is to produce the diffraction pattern slightly off axis, and the zero order may then be removed by spatial filtering if required. Alternatively, other techniques exist to minimize the impact of the zero order light, for example, by causing it to diverge such that it gives only background illumination in the image plane either by including a physical diverging lens in the system [19], or by calculating a kinoform (or hologram phase map) that achieves the same result [27]. Calculating a kinoform to give destructive interference has also been demonstrated as a solution [28]. To minimize the effects of the speckled intensity distribution, the dynamic nature of the device in combination with the relatively long dwell time required for machining enables the simple application of a technique to reduce the speckle contrast, as discussed below.

3. Speckle Reduction Techniques

An inherent problem with phase-only holograms, such as those produced using spatial light modulators, is the speckled intensity distribution of the image. This is a result of interference between the overlapping point spread function of adjacent spots in the image plane. The randomness of the phase in the region between points causes random variations in intensity perceived as speckle noise. A standard approach to reduce speckle contrast is to modulate the speckle pattern in some way and time-average the image. This approach is used in laser projectors in which multiple images with identical amplitudes but independent phase are displayed within a single video frame. These images are displayed at a rate faster than the response time of the eye so the perception is of a single image with reduced speckle contrast. Further improvements can be made using some kind of mechanical modulation within the system, such as a moving diffuser [24]. Such techniques can be easily applied to ns laser machining provided that multiple pulses are used, as is typically the case.

One approach to achieve identical images with varying phase is to use random and statistically independent phase distributions when calculating the kinoform [25]. By combining a number, N, of images each with different phase but identical amplitude, a reduction in the speckle contrast of $1/\sqrt{N}$ will be achieved [29]. A less computationally intensive approach is to calculate a single kinoform and then produce a series of copies that are cyclically shifted in the horizontal and/or vertical planes as illustrated in Fig. 2. Shifting the kinoform in this way does not affect the amplitude distribution of the image but does vary the speckle distribution. These shifts may be performed randomly and, in such a case if, for example,

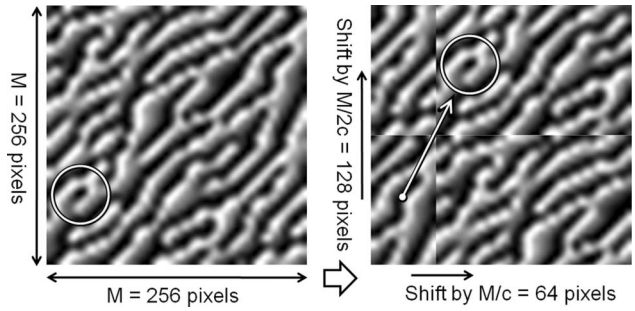

Fig. 2. Demonstration of a periodic kinoform shift for a periodicity $c = 4$. The phase map is shifted by one period in the horizontal axis and two in the vertical axis. The circle tracks a single feature.

16 patterns are combined, a reduction in the speckle contrast of $1/4$ is expected in the resultant image. However, it can be shown mathematically [26] that a deterministic choice of shift distance will meet the requirement that the summation of interference patterns cancel exactly. In practice this requires a series of periodic shifts in orthogonal planes and in principle this approach can completely eliminate the effect of speckle noise in the combined image.

The shifted kinoform approach is simple and effective to implement, and we have implemented this first with randomly selected shift distances and a second time with deterministically selected shift distances. The selection of kinoforms for the deterministic approach [26] is as follows. For a kinoform with $M \times M$ pixels the number of shift periods, c must be selected where c is an integer $\leq M$. The original kinoform is then shifted along one axis by a distance M/c pixels to generate a new kinoform. This is repeated to give c distinct kinoforms. Each of these kinoforms are then shifted by M/c pixels in the orthogonal axis to give c^2 kinoforms in total. For the results shown in the following section, $M = 256$ and $c = 4$, hence, 16 images are required to implement the deterministic-shift approach in this instance. To provide a comparison the same technique is applied separately for 16 randomly chosen shift distances.

Camera images of the beam profile at focus shown in Fig. 3 illustrate the effectiveness of this technique; the pattern generated here is off axis and the zero

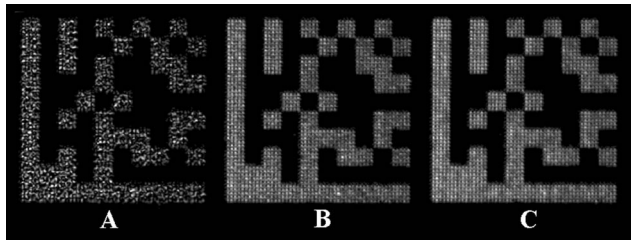

Fig. 3. Images of holograms formed at the end of a 6-f optical system taken using a CCD camera. A, result for the original calculated kinoform. B, 16 images taken for randomly shifted kinoforms, combined and normalized in software. C, 16 images taken for periodically shifted kinoforms, combined and normalized in software.

diffraction order is blocked off. It should also be noted that the starting image used to calculate the phase pattern consisted of 50 × 50 pixels as a small final image size was desired. Consequently, the pixelation is apparent in the holograms. Figure 3A shows the image generated from the original calculated phase pattern, which is highly speckled in nature. Figures 3B and 3C are combined images generated from randomly and periodically shifted phase patterns, respectively. Although pixelation is still apparent, the speckle contrast is reduced significantly. Figure 4 shows the distribution of intensity values within a section of each image, normalized to a maximum pixel value of 255. The dotted curve in Fig. 4 shows the case where each pixel element within the hologram image has been adjusted to the same peak intensity representing the best case intensity distribution with zero speckle contrast but with a pixelated image. The dashed curve illustrates the ideal case where the speckle contrast is zero and there is no pixelation. Pixelation in the reproduced image corresponds directly to the pixels in the initially defined image used to calculate the phase profile. The randomly shifted phase approach gives a significant improvement in uniformity in the reproduced image compared to the single image produced from a single phase profile, and the periodically shifted phase approach gives further improvement.

4. Results

A. Laser Marking Results

Experiments were carried out with the laser operating at full power and at a repetition rate of 15 kHz in order to maximize the intensity available at the workpiece. Marks were made using varying dwell times at fixed locations on the surface to achieve the best possible results. There was no relative motion between the laser focus and the workpiece during the marking process. The average optical power incident on the SLM was approximately 12 W; however, only

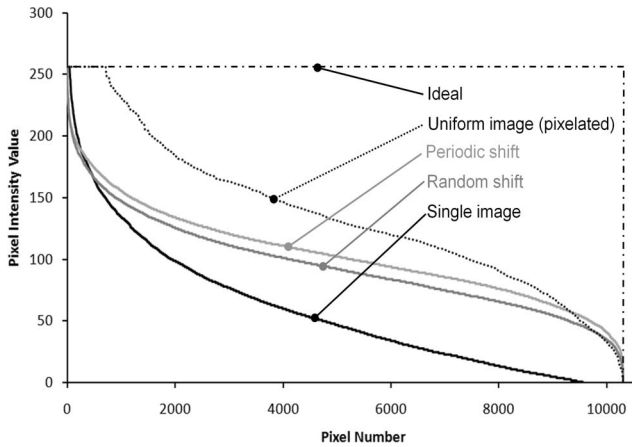

Fig. 4. Plot of normalized intensity values taken from each image shown in Fig. 3. Plots are also shown for the ideal case and for the case where the image is still pixelated but each pixel is of uniform intensity.

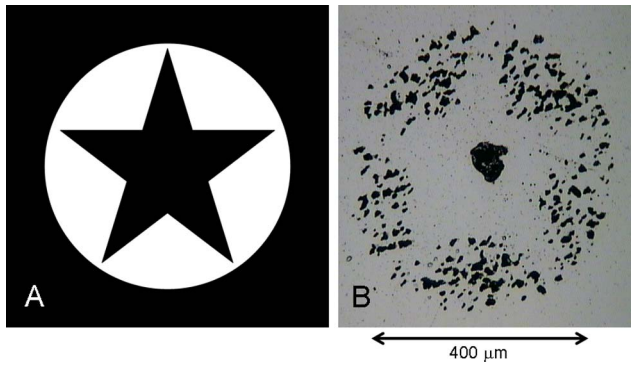

Fig. 5. A, star pattern used to derive kinoform for hologram. B, star pattern marked on thin layer of aluminum coated on glass. A kinoform was marked nine times with 100 ms exposure.

~3.5 W was delivered to the image on the workpiece. This includes losses due to the diffraction efficiency of the device with the specific addressed pattern as well as other losses in the optical system, including reflection losses from optical components and the reflectivity of the SLM.

Figure 5 shows an initial attempt at marking using the SLM. Figure 5A shows the image used as a starting point to calculate a single kinoform to display on the SLM. Figure 5B shows the result of marking this pattern on a thin aluminum film coated on glass, using nine exposures of 100 ms each. The dark areas in the image are where the film has been removed exposing the dark (unlit) glass underneath. The mark caused by the zero diffraction order is prominent in the center of the image.

In Fig. 6, the same star pattern has been marked; however, this time the pattern is off axis to disassociate it from the zero order. While in each case a mark was left on the surface by the zero order, similar to that seen in Fig. 5, this mark is separate from the image (and not seen in the figure). Each image in Fig. 6 was marked by 16 exposures of 200 ms each. However, the kinoforms used vary in each case. In Fig. 6A, a single kinoform was used and, consequently, the image is highly speckled. For the results shown in Fig. 6B, the original kinoform was taken and shifted randomly 16 times as described in the previous section to modulate the speckle profile. Each of these patterns was marked once and the

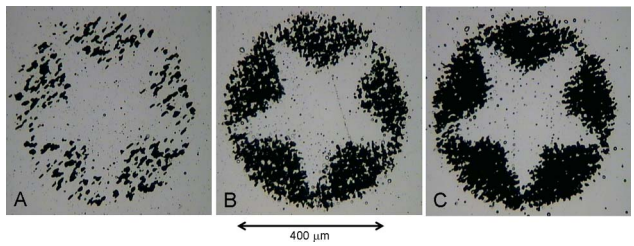

Fig. 6. Marks on a thin layer of aluminum coated on glass created using an SLM to produce an off-axis image. A, single kinoform marked 16 times with 200 ms exposure. B, 16 randomly shifted kinoforms marked for 200 ms each. C, 16 periodically shifted kinoforms marked for 200 ms each.

combined result shows a significantly reduced speckle contrast and a clearer image. The same approach was taken to produce Fig. 6C. However, this time the shifts were periodic, producing some further improvement in the speckle contrast.

Slightly more complex patterns are demonstrated in Fig. 7. Figure 7A shows a 10×10 data matrix pattern representing the letter "A", again marked on a layer of aluminum coated on glass. Sixteen periodically shifted kinoforms were used to make up the image, each marked for 10 ms. For this image, 5×5 pixels were used for each element in the matrix, the minimum number of pixels that can be used while maintaining a reasonable quality reconstruction. Figure 7B shows a similar pattern marked in photoresist. In this case 16 periodically shifted kinoforms were marked for 300 ms each to make up the image. A mark from the zero order is apparent in the bottom right corner. A larger area pattern is feasible as the photoresist is more easily removed by the laser due to its characteristic material properties, specifically, increased optical absorption and lower melting/vaporization points and lower thermal mass. The metal underneath the pattern is unaffected by the process due to its higher machining threshold.

In terms of quality, both marks in Fig. 7 are clearly defined with sharp edges. Some pixilation is apparent in Fig. 7A as well as a fading of the mark toward the top of the shape. This is a result of the slightly nonuniform intensity gradient in the diffraction image used for marking. Because of the high optical intensity required to machine a metal combined with a high thermal conductivity, it is necessary to strike a balance between over marking the lower portion of the image and under marking the top. In Fig. 7B the larger scale image in photoresist does not show this gradient. Because of the lower machining threshold and larger scale, machining can continue until all of the resist is removed in the desired regions without causing noticeable thermal damage at the edges of the mark.

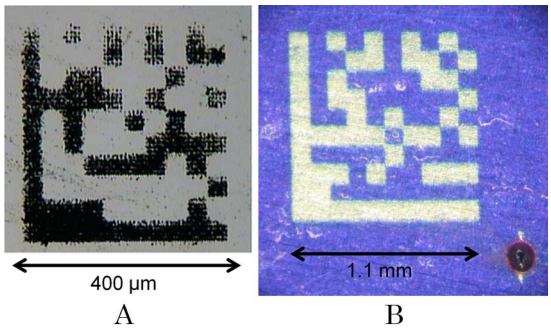

Fig. 7. (Color online) A, data matrix pattern representing character "A" marked on thin layer of aluminum coated on glass. 16 periodically shifted kinoforms were marked for 10 ms each. B, data matrix marked in photoresist using 16 periodically shifted kinoforms marked for 300 ms each. The stainless steel substrate is untouched by the machining process.

B. Reduced Mark Size

Clearly machining photoresists and metal films has a limited number of useful applications, whereas, the ability to machine bulk materials would open up a wider range of applications. Thin films are relatively easy to machine due to their low thermal mass. In the ns regime material is removed by a combination of evaporation and melting. Because of the intensity available to mark the relatively wide area patterns shown in this work the machining processes presented here tend toward a thermal melting process rather than ablation. When machining bulk materials, the greater thermal mass in the component results in heat being conducted away from the mark during the machining process, thus, making the process less efficient. The best way to overcome this problem is to increase the laser intensity, and as we are already working at the maximum available power this means making the shape smaller.

To achieve this, the final lens of the system was replaced with initially a 50 mm focal length singlet lens and subsequently a 30 mm focal length doublet. As the focal length becomes shorter in relation to the beam diameter, the use of a doublet lens is required to minimize aberrations in the image. Figure 8A shows a mark of 370 μm width made using the 50 mm lens on stainless steel. The surface was polished mechanically using silicon carbide polishing papers down to 4000 grit before the mark was generated and some lines are apparent from this polishing. Although the data matrix mark is readable, it is apparent that the individual squares are starting to blur together, resulting from the thermal nature of the process and the spread of heat over the relatively long marking times. Figure 8B shows a smaller scale mark of 200 μm width, also on polished stainless steel, made using the 30 mm doublet lens. To

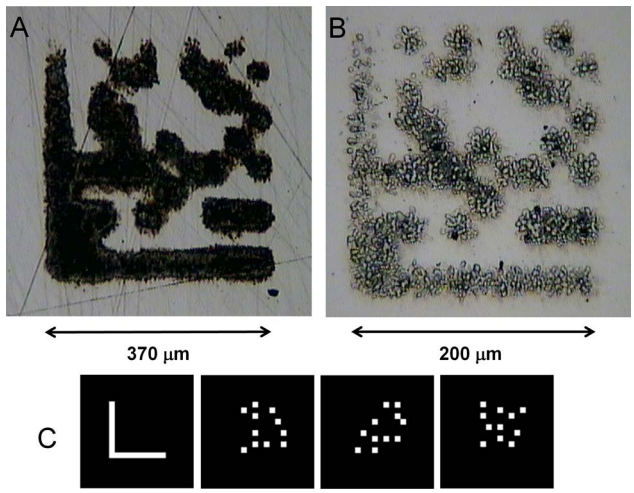

Fig. 8. Data matrix representing the letters "AOP" marked on stainless steel. A, using a 50 mm single element lens and 16 periodically shifted kinoforms marked for 100 ms each. B, using a 30 mm doublet lens four overlapping patterns are marked using a total of 36 periodically shifted kinoforms each marked for 1.7 ms. C, four separate patterns used to build up the mark shown in B.

minimize the thermal spread, this mark was built up from four different patterns shown in Fig. 8C. With the exception of the bracket, the code was split up such that no two squares were marked adjacent to each other at the same time. In this instance the shape was divided up manually; however, this could conceivably be achieved using a computer algorithm. The disadvantage is an increase in computation time to split the shape and produce three phase profiles instead of one (the phase profile required to generate the bracket being standard for each code). The periodicity of the speckle reduction process was reduced from four to three to reduce the number of different phase patterns used to nine for each frame. In total, 36 different frames were marked, but for only 1.7 ms each. By reducing the area marked both by reducing the image size and by splitting the shape into parts that are marked separately, the laser intensity on the surface during marking is increased significantly enabling a reduction in machining time from 100 ms per phase pattern to 1.7 ms. Taking the thermal diffusivity of stainless steel as $4.2 \times 10^{-6}\,\mathrm{m}^2/\mathrm{s}$, an estimate of the thermal diffusion length over the marking time can be made of $\sim 20\,\mu$m in Fig. 8A compared to just $3\,\mu$m in Fig. 8B. These numbers appear broadly consistent with the extent of the heat-affected region in each image. Reducing the size of the mark further would result in increased intensity and, therefore, reduced marking time and reduced extent of the heat-affected zone.

The shape in Fig. 8B is clearly defined, although the edges are not perfectly sharp. The pattern is easily decoded using appropriate readily available software. This demonstrates that the mark is fit for purpose as a discrete tracking mark that may be applied to a variety of items.

With the goal of achieving the smallest mark possible there are two primary limitations. First, the ability of the optical system to generate an image of sufficient resolution and uniformity, and second, the requirement for sufficient optical intensity to mark the surface without thermal effects in the material degrading the mark quality. In practice, the limiting factor on the size of the image is the numerical aperture (NA) of the final lens. Clearly, a shorter focal length will give a smaller image. However, if the lens diameter is too small, then information is lost and the reconstructed image deteriorates. The $30f$ doublet used here had an NA of $0.423\,rad$, which represents the optimum for commercially available off-the-shelf components. For a given image size the mark quality may be improved by reducing the machining time in order to reduce the heat-affected zone around the mark. This may be achieved by increasing the laser intensity, which would require changing to a higher power and/or shorter pulse length laser system, adding significantly to cost, or improving the efficiency of the optical system, the least efficient component being the SLM itself. Clearly, reducing the mark area also increases the intensity and can reduce thermal effects.

Because of the limitations in intensity, the machining results that are possible with the SLM are limited to small-scale (submillimeter) marks in bulk metal surfaces or slightly larger marks in more easily machined materials, such as photoresists. Discrete small-scale marks are of value as a means to provide traceability of high-value items and this is one possible area in which the SLM could offer an advantage, enabling distinct codes to be generated rapidly. Alternatively, the device could be useful in developing a process that requires a fixed diffractive optic, enabling quick realization of iterations in a design process. In conjunction with a scan head system the SLM could be applied to surface structuring or patterning. One application of such an approach would be the direct writing of etching masks in photoresist, thus avoiding the developing stage.

5. Summary

A spatial light modulator has been used in conjunction with a high repetition rate ns laser operating at 12 W average power and applied to marking applications on thin films and bulk metal surfaces. The speckled intensity distribution across the image generated by the device limits the quality of the marking result that may be achieved. However, this has been overcome by applying a periodic technique to create a series of modified kinoforms. The summation of the resultant images gives a result with a close to uniform intensity distribution, which can be realized on a workpiece by sequentially marking with each kinoform and can be achieved in a short time period. This technique dramatically improves the quality of marks produced compared to marking with a single kinoform. Further improvements in the marking quality have been demonstrated for data matrix marks at small scales by using the dynamic nature of the device to mark groups of nonadjacent elements sequentially, thus minimizing the spread of heat between adjacent elements that would otherwise reduce the resolution of the mark.

Machining of thin metal films and photoresist has been demonstrated at scales of around 1 mm and could potentially be used for generating small-scale structures and direct writing of etching masks. Small-scale structures are also feasible with feature sizes around $20\,\mu$m, which could, for example, provide traceability of high-value parts for which small marking dimensions are often an advantage.

This work was funded through the Heriot-Watt Innovative Manufacturing Research Centre (IMRC) (EP/F02553X) with industrial support and funding from Renishaw plc.

References

1. A. Bich, J. Rieck, C. Dumouchel, S. Roth, K. J. Weible, M. Eisner, R. Voelkel, M. Zimmermann, M. Rank, M. Schmidt, R. Bitterli, N. Ramanan, P. Ruffieux, T. Scharf, W. Noell, H. P. Herzig, and N. de Rooij, "Multifunctional micro-optical elements for laser beam homogenizing and beam shaping," Proc. SPIE **6879**, 68790Q (2008).

2. A. Laskin, *Beam Shaping? Easy!* (Industrial Laser Solutions, 2006), pp. 17–19.
3. E. Neiss, M. Flury, and J. Fontaine, "Diffractive optical elements for laser marking applications," Proc. SPIE **7003**, 70032L (2008).
4. T. Kajava, A. Hakola, H. Elfstrom, J. Simonen, P. Paakkonen, and J. Turunen, "Flat-top profile of an excimer-laser beam generated using beam-splitter gratings," Opt. Commun. **268**, 289–293 (2006).
5. T. Lizotte and O. Ohar, "Structured beam shaping for precision laser dicing of multilayered substrates," Proc. SPIE **6458**, 64580X (2007).
6. J. Ihlemann and K. Rubahn, "Excimer laser micro machining: fabrication and applications of dielectric masks," Appl. Surf. Sci. **154**, 587–592 (2000).
7. S. Campbell, S. M. F. Triphan, R. El-Agmy, A. H. Greenaway, and D. T. Reid, "Direct optimization of femtosecond laser ablation using adaptive wavefront shaping," J. Opt. A Pure Appl. Opt. **9**, 1100–1104 (2007).
8. R. J. Beck, R.Carrington, J. P. Parry, W. N. MacPherson, A. Waddie, D. T. Reid, N. Weston, J. D. Shephard, and D. P. Hand, "Adaptive optics for optimization of laser processing," in *Proceedings of LAMP2009—the 5th International Congress on Laser Advanced Materials Processing* (2009), paper 09-018.
9. J. C. Sinquin, J. M. Lurcon, and C. Guillemard, "Deformable mirror technologies for astronomy at CILAS," Proc. SPIE **7015**, 70150O (2008).
10. I. Murokh, A. Kerner, and S. Filatov, "Laser marking using a digital micro-mirror device," U.S. patent 6,836,284 (28 December 2004).
11. E. T. Ritschdorff and J. B. Shear, "Multiphoton lithography using a high-repetition rate microchip laser," Anal. Chem. **82**, 8733–8737 (2010).
12. A. Bertsch, S. Zissi, J. Y. Jezequel, S. Corbel, and J. C. Andre, "Microstereophotolithography using a liquid crystal display as dynamic mask-generator," Microsyst. Technol. **3**, 42–47 (1997).
13. V. Laude, "Twisted-nematic liquid-crystal pixelated active lens," Opt. Commun. **153**, 134–152 (1998).
14. E. Martin-Badosa, M. Montes-Usategui, A. Carnicer, J. Andilla, E. Pleguezuelos, and I. Juvells, "Design strategies for optimizing holographic optical tweezers set-ups," J. Opt. A Pure Appl. Opt. **9**, S267–S277 (2007).
15. K. D. Wulff, D. G. Cole, R. L. Clark, R. DiLeonardo, J. Leach, J. Cooper, G. Gibson, and M. J. Padgett, "Aberration correction in holographic optical tweezers," Opt. Express **14**, 4169–4174 (2006).
16. P. M. Prieto, E. J. Fernandez, S. Manzanera, and P. Artal, "Adaptive optics with a programmable phase modulator: applications in the human eye," Opt. Express **12**, 4059–4071 (2004).
17. M. Pospiech, M. Emons, A. Steinmann, G. Palmer, R. Osellame, N. Bellini, G. Cerullo, and U. Morgner, "Double waveguide couplers produced by simultaneous femtosecond writing," Opt. Express **17**, 3555–3563 (2009).
18. L. Kelemen, S. Valkai, and P. Ormos, "Parallel photopolymerisation with complex light patterns generated by diffractive optical elements," Opt. Express **15**, 14488–14497 (2007).
19. Z. Kuang, D. Liu, W. Perrie, S. Edwardson, M. Sharp, E. Fearon, G. Dearden, and K. Watkins, "Fast parallel diffractive multi-beam femtosecond laser surface micro-structuring," Appl. Surf. Sci. **255**, 6582–6588 (2009).
20. A. T. Sandstrom, A.-K.Holmer, U. Lungblad, and D. Hanstorp, "Pattern generation system using a spatial light modulator," U.S. patent 6,700,095 (2 March 2004).
21. D. L. Chen, Y. Zhang, A. Feng, Z. Xu, B. Li, and H. Shen, "Investigation of laser marking technology with the image mask of liquid crystal display," Appl. Mech. Mat. **43**, 633–636 (2011).
22. F. Ghauri, "Method and system for laser-based high-speed digital marking of objects," U.S. patent application 20100054287 (4 March 2010).
23. R. J. Beck, J. P. Parry, W. N. MacPherson, A. Waddie, N. J. Weston, J. D. Shephard, and D. P. Hand, "Application of cooled spatial light modulator for high power nanosecond laser micromachining," Opt. Express **18**, 17059–17065 (2010).
24. E. Buckley, "Holographic laser projection technology," in *SID Symposium Digest* (Society for Information Display, 2008), Vol Xxxix, Books I–III, pp. 1074–1078.
25. J. Amako, H. Miura, and T. Sonehara, "Speckle-noise reduction on kinoform reconstruction using a phase-only spatial light-modulator," Appl. Opt. **34**, 3165–3171 (1995).
26. L. Golan and S. Shoham, "Speckle elimination using shift-averaging in high-rate holographic projection," Opt. Express **17**, 1330–1339 (2009).
27. M. Polin, K. Ladavac, S. H. Lee, Y. Roichman, and D. G. Grier, "Optimized holographic optical traps," Opt. Express **13**, 5831–5845 (2005).
28. D. Palima and V. R. Daria, "Holographic projection of arbitrary light patterns with a suppressed zero-order beam," Appl. Opt. **46**, 4197–4201 (2007).
29. J. W. Goodman, "Some fundamental properties of speckle," J. Opt. Soc. Am. **66**, 1145–1150 (1976).